Elisha *et al. Collagen and Leather* (2026) 8:16
https://doi.org/10.1186/s42825-026-00248-7

Collagen and Leather

RESEARCH Open Access

ACE inhibitory and DPP-IV inhibitory activity of collagen peptides derived from the snapper salmon (*Otolithes ruber*) skin collagen via papain and pepsin-trypsin hydrolysis

Cherise Elisha[1], Prashant Bhagwat[1*], Ayodeji Amobonye[1,2] and Santhosh Pillai[1]

Abstract
Fish-based collagen supplements have potential health benefits, including antioxidant, ACE inhibitory, and DPP-IV inhibitory properties, which are expressed upon their digestion in the gastrointestinal system, thus releasing bioactive peptides (BPs). This study evaluated the pre-digestion of fish collagen using papain as a pre-digestive enzyme, which has broad specificity to enhance collagen breakdown and BPs release. Fish skin collagen was extracted via acid solubilisation, confirmed as type-I, and subsequently hydrolysed using two methods: pepsin-trypsin digestion (PTD) and pre-digestion with papain followed by PTD (PDPTD). The PDPTD–fish collagen hydrolysates (FCH) exhibited IC50 values (mg/mL) of 0.088 for ACE, 1.67 for DPP-IV, as well as 2.38 and 0.026 for antioxidant activities including DPPH and ABTS radicals scavenging, respectively, which were significantly lower than that of PTD-FCH. The FCH (PTD and PDPTD) were identified using LC-MS/MS analysis, and molecular docking studies showed lower binding energies for PDPTD–FCH peptides, particularly IGFPGFPG, against ACE (-11.2 kcal/mol) and DPP-IV (-9.1 kcal/mol), suggesting better inhibitory ability exhibited by BPs. This study highlighted fish collagen as a valuable source of BPs with enhanced bioactivity when pre-digested with papain, indicating its potential for functional foods and nutraceutical industries.

Keywords Fish collagen, Antioxidant peptides, Antihypertensive and antidiabetic potential, Functional foods, Nutraceuticals

*Correspondence:
Prashant Bhagwat
pkbhagwat9988@gmail.com; prashantb@dut.ac.za

Full list of author information is available at the end of the article

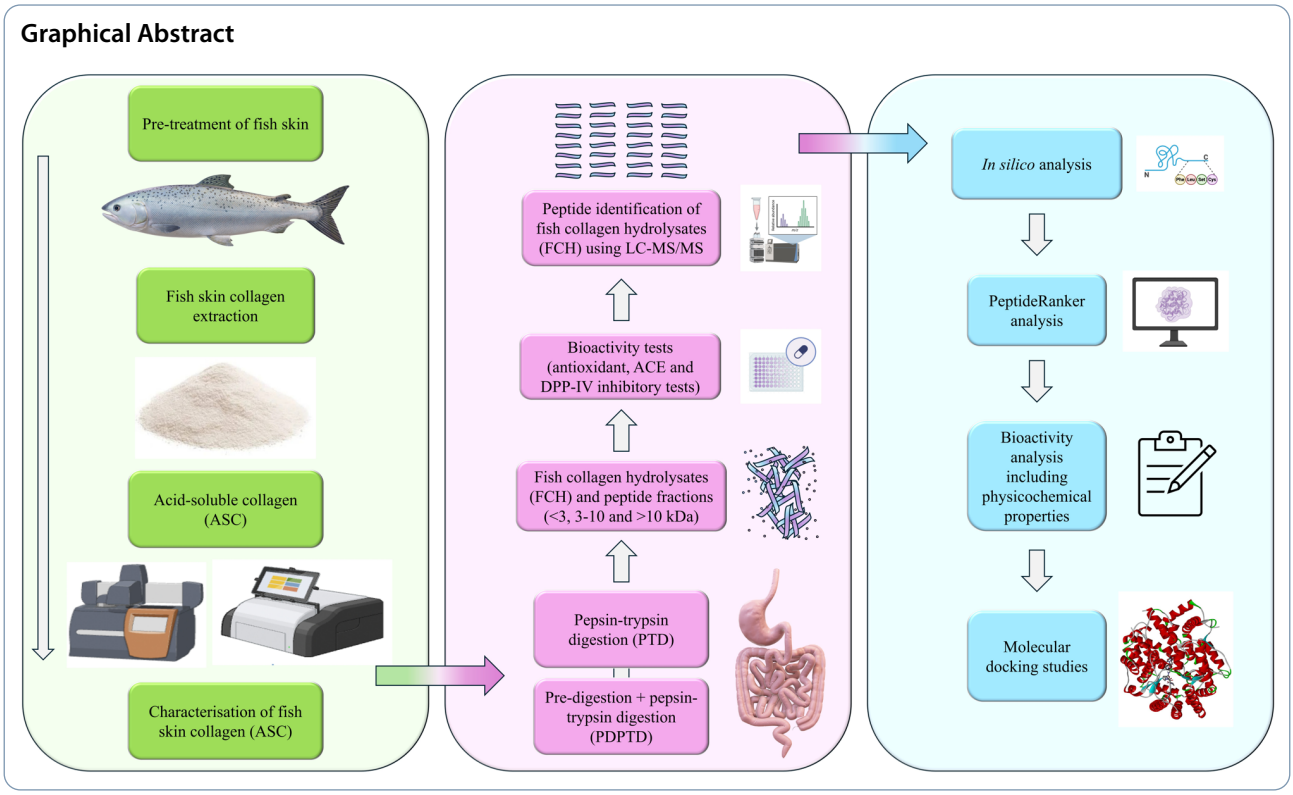

1 Introduction

Collagen is a fibrous structural protein with a molecular weight of ~ 300 kDa and is regarded as the predominant component of the animal structural matrix, accounting for ~ 30% of their total protein content [1]. Collagen and its derivatives have a high commercial value in the food, cosmetics, and pharmaceutical industries due to their high biodegradability and biocompatibility [2–4]. Although bovine and porcine collagen sources are widely used in various industries, health concerns (such as bovine spongiform encephalopathy and foot-and-mouth disease) along with religious and cultural restrictions have driven demand for alternative collagen sources [5]. Marine-derived collagen has gained significant attention recently due to its abundance, biocompatibility, high commercial value, and disease-free nature [6]. In addition, its alignment with diverse religious and cultural practices has enabled its broad applications in various industries [4, 7]. Interestingly, marine-based collagen can be derived from fish waste such as skin, bones, and scales, which is frequently thrown into landfills, a process that has resulted in major environmental pollution and unpleasant odours [8]. Hence, the efficient recovery of collagen presents opportunities for upcycling fish waste into value-added products with high bioavailability, biodegradability, and zero toxicity, thereby contributing to cleaner production and sustainable resource management [9]. Moreover, the extracted collagen can be broken down to release bioactive peptides (BPs), thereby enhancing its functional and commercial potential [2, 10].

BPs are small protein fragments with 2–20 amino acid sequences that are known to exhibit various health-benefiting properties, including antioxidant, antihypertensive, and antidiabetic activities [11–13]. The biological activities of peptides derived from fish collagen vary with their amino acid composition, thus influencing their functional properties and potential health benefits [14]. Various methods of generating these BPs have been reported, including enzyme proteolysis and microbial fermentation [15, 16]. The enzyme hydrolysis process is extremely efficient and rapid, and it has been noted to reduce allergenicity, improve the physicochemical, nutritional, and functional properties of the hydrolysed proteins, and generate hydrolysates containing conserved peptides [17, 18].

In mammals, dietary proteins get hydrolysed by a highly specialised digestive system comprising major proteases such as pepsin and trypsin. Interestingly, pre-digestion of a protein with an exogenous protease, distinct from digestive proteases, may facilitate the release of peptides with enhanced bioactivity. Considering this, the current study evaluates the pre-digestion of fish collagen before subjecting it to in vitro pepsin-trypsin digestion. Since collagen has already been partially broken down by pre-digestion, this approach can produce a greater number of BPs and allows for a higher efficiency

in the digestibility process. In this regard, papain was selected as the pre-digestive enzyme. Papain belongs to the cysteine protease family and cleaves peptide bonds in the middle of the protein chain, adjacent to amino acids with aromatic or large hydrophobic side chains, such as phenylalanine, tryptophan, and tyrosine [19]. In addition, papain derived from *Carica papaya* offers several advantages, including low cost, biodegradability, and a favourable safety profile. Furthermore, it operates efficiently across a wide pH range (5.0–8.0) and possesses broad cleavage specificity, making it highly suitable for pre-digestion applications [20]. Papain, in combination with other proteases, releases hydrolysates with an increased degree of hydrolysis and enhanced bioactivity [21]. Papain also exhibits significant versatility, functioning effectively within a broad pH range of 4.0 to 10.0 and at temperatures of up to 80 °C. Therefore, papain, combined with digestive enzymes such as pepsin (aspartic protease with a broad cleavage specificity) and trypsin (serine protease that cleaves peptide bonds at the carboxyl side of lysine and arginine), was employed to generate potential BPs from fish collagen.

To the best of our knowledge, this is the first study that evaluates the synergy of pre-digestion using papain, together with pepsin-trypsin digestion to generate fish collagen BPs with a wider range of potential bioactivities such as angiotensin-converting enzyme (ACE) , dipeptidyl peptidase-IV (DPP-IV) inhibitory, and antioxidant activities using in vitro assays. The potential BPs were further identified using liquid chromatography-tandem mass spectrometry (LC-MS/MS), followed by in silico assessments to confirm the most potent peptides. This study hypothesises that pre-digestion of fish collagen with papain, followed by sequential pepsin–trypsin hydrolysis, will enhance the antioxidant, ACE inhibitory, and DPP-IV inhibitory activities of the resulting peptides compared to pepsin–trypsin digestion alone.

2 Materials and methods

2.1 Materials and reagents

Fresh snapper salmon (*Otolithes ruber*) was purchased from a local seafood market in Durban, South Africa. Sodium hydroxide, butyl alcohol, acetic acid, hydrochloric acid, papain (≥ 3 U/mg; 76220), pepsin (≥ 400 U/mg; P7125), trypsin (1500 U/mg; T4799), commercial calf skin collagen (CSC) (C9791), DPPH (2,2-diphenyl-1-picrylhydrazyl), and ABTS [2,2′-azinobis(3-ethylbenzothiazoline-6-sulfonic acid)] were all purchased from Sigma-Aldrich (USA). All reagents used in this study were of analytical grade.

2.2 Extraction and characterisation of fish skin collagen

The snapper salmon (*Otolithes ruber*) fish skin was pretreated according to Bhuimbar et al. [2]. Briefly, the fish skin was pretreated in 0.1 M NaOH (1:15 *w/v*) for 48 h, washed twice with distilled water, and suspended in 10% butyl alcohol (1:15 *w/v*) for 24 h. Thereafter, the fish skin was washed twice with distilled water to remove the butyl alcohol. The pretreated fish skin was further suspended in 0.5 M acetic acid (1:30 *w/v*) for 72 h with continuous stirring at 4 °C. The fish skin was then squeezed and filtered using a muslin cloth, followed by centrifugation (10,000 × *g*, 4 °C). The filtrate was precipitated by adding 1 M NaCl and placed at 4 °C overnight. Subsequently, the solution was centrifuged at 10,000 × *g* for 15 min at 4 °C, and the resulting precipitate was re-extracted in 0.5 M acetic acid. The acid-soluble collagen was then dialysed against distilled water for 48 h. The final dialysate was freeze-dried and regarded as acid-soluble collagen (ASC).

2.3 Biochemical and biophysical characterisation of ASC

The extraction yield of ASC was calculated on a dry weight basis according to Faralizadeh et al. [22]. Ultraviolet-visible spectroscopy (200 to 400 nm) of the ASC was determined using the Shimadzu UV-1280 spectrophotometer following the method of Pal and Suresh [23]. Thereafter, the ASC was analysed using Fourier transform infrared spectroscopy (FT-IR) (Agilent Cary 630 FTIR) at 400–4000 cm^{-1} range [2]. The thermal stability of the ASC was calculated by estimating the endothermic peak, denaturation temperature (Td), and melting temperature (Tm) using a differential scanning calorimeter (DSC) (DSC 25, Discovery series, TA Instruments, New Castle, United States) [24]. The thermal stability analysis was conducted at a temperature range of 30–250 °C and a scanning rate of 10 °C/min. Thereafter, a circular dichroism (CD) spectropolarimeter (Chirascan-Plus, Applied Photophysics, Leatherhead, UK) was used to analyse the secondary structure of the extracted ASC. The sodium dodecyl sulphate-polyacrylamide gel electrophoresis (SDS-PAGE) pattern of extracted ASC was performed according to Laemmli [25] using an 8% resolving and 4% stacking gel. A high molecular weight protein marker (11–250 kDa, Sigma-Aldrich, USA) was used to estimate the molecular weight of the protein. The gel was stained using 0.2% (*w/v*) Coomassie brilliant blue R250 followed by destaining with 50% (*v/v*) methanol with 10% (*v/v*) acetic acid. Additionally, amino acid analysis was conducted by hydrolysing 100 mg of the ASC at 110 °C for 18 h in 0.5 ml of 6 M HCl, according to Kulkarni et al. [26]. Commercial CSC was used as a standard throughout the characterisation of ASC.

2.4 Preparation of fish collagen hydrolysates (FCH) and peptide fractions

2.4.1 In vitro pre-digestion and pepsin-trypsin digestion

The extracted fish skin collagen, ASC, was hydrolysed using papain from *Carica papaya*. The pre-digestion step

was performed according to Liao et al. [27] with slight modifications. Briefly, papain (≥ 3 U/mg, 1%, *w/w*) was added to the fish collagen solution (5%, *w/v*) and adjusted to pH 6.0. The hydrolysis was carried out at 60 °C for 5 h, and the enzyme was inactivated by heating at 100 °C for 20 min, cooled to room temperature and centrifuged at 6000 × *g* for 10 min at 25 °C. The resulting supernatant was further subjected to in vitro pepsintrypsin digestion (PDPTD). The simulated gastric juice was prepared with 0.2% (*w/v)* NaCl, 0.32% (*w/v*) pepsin from porcine gastric mucosa, and 0.7% (*v/v*) HCl in distilled water (pH of 3.0), and incubated for 4 h (37 °C at 150 rpm). Subsequently, the digests were further adjusted to pH 6.8, followed by the addition of 0.7% (*w/v*) trypsin and incubated for 6 h under the same conditions. The pepsin and trypsin in the digests were inactivated by boiling in a water bath for 10 min and centrifuged at 10 000 × *g* for 30 min. In addition, a control group was set up using fish collagen without pre-digestion, regarded as PTD (pepsin-trypsin digestion only). The resulting supernatants were then subjected to peptide fractionation.

2.4.2 Peptide fractionation

The FCH from both the test and control groups were then fractionated into < 3, 3–10, and > 10 kDa peptides using molecular weight cut-off membranes (Amicon® Ultra Centrifugal Filter, Sigma-Aldrich, USA), freeze-dried, and stored at -20 °C. Before fractionation, FCH were also freeze-dried and used for further bioactivity analyses with the peptide fractions.

2.5 Bioactivity analyses of FCH and peptide fractions

The freeze-dried peptide fractions and FCH were analysed for various bioactivities including antihypertensive potential using ACE inhibition assay, antidiabetic potential using DPP-IV inhibition assay, and antioxidant potential using DPPH radical scavenging assay as well as ABTS scavenging assay. ACE inhibitory activity was evaluated using the ACE activity assay kit (CS0002 Sigma-Aldrich, USA) by hydrolysing angiotensin I to produce active angiotensin II. It employs a synthetic fluorogenic peptide as the substrate, with the resulting fluorescence directly proportional to ACE activity. Various concentrations of freeze-dried FCH released during PDPTD and PTD (1–10 mg/mL) were prepared, out of which 10 µL of the respective concentration was added to the black 96-well plates (Thermo Fisher, Waltham, MA, USA). Thereafter, 40 µL of ACE enzyme and 50 µL of fluorogenic substrate were added. The reaction was carried out at 37 °C and fluorescence was read every minute for 5 min in the Varioskan Lux microplate reader (Thermo Fisher). In a subsequent investigation, a DPP-IV inhibitor screening kit (MAK203 Merck, USA) was used to conduct the DPP-IV inhibitory activity assay of the peptide fractions and FCH. Similarly, various concentrations of freeze-dried FCH released during PDPTD and PTD (0.1–10 mg/mL) were prepared, out of which 25 µL of the respective concentration was added to the black 96-well plates (Thermo Fisher). Thereafter, 50 µL of enzyme solution was added, mixed, and incubated at 37 °C for 10 min, followed by the addition of the DPP-IV substrate (25 µL). The fluorescence (FLU, λex = 360 nm / λem = 460 nm) was measured at 37 °C with the Varioskan Lux microplate reader (Thermo Fisher). The peptide fractions and FCH derived from PDPTD and PTD were tested at various concentrations of 0.1–10 mg/mL, and the relative DPP-IV inhibition (%) was calculated as follows [(FLU_1 and FLU_2 = fluorescence readings at times T_1 and T_2, respectively; T_1 and T_2 = time points (min)]:

$$\text{Slope} = \frac{(\text{FLU2} - \text{FLU1})}{(\text{T2} - \text{T1})} = \text{FLU/min} \quad (1)$$

$$\text{DPP} - \text{IV inhibition}\,(\%) = \frac{\text{T2} - \text{T1}\,(\text{Sample})}{(\text{T2} - \text{T1})\,(\text{Negative control})} \quad (2)$$

Furthermore, the DPPH radical scavenging activity was determined according to Nurilmala et al. [12] with FCH and peptide fractions (1–10 mg/mL) from both PDPTD and PTD, which were suitably diluted. DPPH solution (100 µL, 0.1 mM in 95% methanol) was mixed with 100 µL of FCH solution from PDPTD and PTD (0.01–0.1 mg/mL) and incubated in the dark at room temperature for 45 min. The absorbance of the incubated solution was read at 517 nm using the Thermo Scientific Multiskan GO microplate reader (Thermo Fisher). The ABTS radical scavenging activity was determined according to the method of Re et al. [28] with slight modifications. A 20 µL aliquot of peptide fractions and FCH (PDPTD and PTD) at various concentrations (0.01–0.1 mg/mL) was mixed with 180 µL of the ABTS solution, and the free radical scavenging capacity of the peptides was measured. The antioxidant activity of the samples was calculated using the following equations:

$$DPPH\ radical\ scavenging\ activity\ (\%) = \frac{Absorption\ of\ control\ -\ Absorption\ of\ sample}{Absorption\ of\ control} \times 100 \quad (3)$$

$$ABTS\ radical\ scavenging\ activity\ (\%) = \frac{Absorption\ of\ control\ -\ Absorption\ of\ sample}{Absorption\ of\ control} \times 100 \quad (4)$$

2.6 LC-MS/MS and in silico analysis of FCH

2.6.1 LC-MS/MS analysis

Liquid chromatography of the FCH (PDPTD and PTD) was performed on the Thermo Scientific Ultimate 3000 RSLC (Thermo Fisher, USA) as per the protocol developed previously in our laboratory [29]. The freeze-dried PDPTD and PTD FCH were analysed to identify peptide sequences at the Central Analytical Facilities (CAF), Stellenbosch University, Stellenbosch, South Africa. Liquid chromatography was carried out on a Thermo Scientific Ultimate 3000 RSLC (Thermo Fisher) with a 5 mm x 300 mm C18 trap column (Thermo Fisher) and a charged surface hybrid (CSH) 25 cm x 75 mm, 1.7 mm particle size C18 analytical column (Waters, Milford, MA, USA). The analytical conditions were as follows: (A) 2% acetonitrile: water; 0.1% formic acid and (B) 100% acetonitrile: water; flow rate: 300 nl/min; gradient: 5.0–30% (B) over 60 min, and 30–50% (B) between 60 and 80 min. Thereafter, mass spectrometry was done using a Thermo Scientific Fusion mass spectrometer (Thermo Fisher) together with a Nanospray Flex ionisation source. The data were collected in positive mode with spray voltage set to 1.8 kV and ion transfer capillary temperature set to 275 °C. MS1 scans were performed using the Orbitrap detector set at 60 000 resolutions over the scan range 375–1500 with automatic gain control (AGC) target set to the standard. MS2 acquisitions were conducted using monoisotopic precursor selection for ions with charges +2 - +7 with error tolerance set to +/-10 ppm. Precursor ions were identified and used for fragmentation in higher-energy collisional dissociation (HCD) mode whilst ensuring that the quadrupole mass analyser with HCD energy was set to 30%. Fragment ions were detected in the Orbitrap mass analyser set to 30 000 resolutions. The AGC target was set to standard and the maximum injection time to 100 ms. The data were attained in centroid mode. Thereafter, PeptideShaker v.2.2.2 was used for data analysis with the following settings: enzyme: pepsin and trypsin; peptide charges from +2 to +4; precursor mass tolerance 10 ppm and fragmentation ion types (b and y). Thereafter, the peptide sequences were identified from the LC-MS/MS analysis following the protocol of Farag et al. [30], which were further subjected to in silico analysis.

2.6.2 PeptideRanker

The potential of the peptides released after PDPTD and PTD of the FCH was predicted using PeptideRanker (http://distilldeep.ucd.ie/PeptideRanker/). Peptides with the high and low bioactivity potential were represented by the maximum score (> 0.5) and the minimum score (< 0.5), respectively. The fish collagen peptides from both PDPTD and PTD, with a peptide ranking of 0.5 and above, were subjected to further analysis [31].

2.6.3 In silico analysis of potential antioxidant, ACE and DPP-IV inhibitory activity

The profiles for the potential biological activity of the FCH peptides were analysed using various prediction software based on the desired bioactivity. First, AnOxPePred (http://services.bioinformatics.dtu.dk/service.php?AnOxPePred-1.0) was used to analyse the peptide sequences for potential antioxidant activity [32]. Thereafter, antihypertensive peptides were analysed using AHTpin (https://webs.iiitd.edu.in/raghava/ahtpin/help.php) [33], and for DPP-IV inhibitory activity, StackDPPIV (https://pmlabstack.pythonanywhere.com/StackDPPIV) was used [34].

2.6.4 Physicochemical properties

Peptides with possible bioactivity, identified using PeptideRanker, were screened for their physicochemical characteristics using PepCalc (http://pepcalc.com/) [35]. The online peptide calculators were employed to assess the physicochemical attributes of the potentially bioactive peptides derived from FCH. Parameters such as theoretical molecular weight, isoelectric point (pI), peptide charge at pH 7.0, estimated solubility, and extinction coefficient of the collagen peptides were evaluated.

2.6.5 Molecular docking studies

The binding properties of the predicted bioactive peptides with the target proteins, viz., ACE, and DPP-IV, were evaluated via rigid molecular docking. Based on the potential bioactivity profiles predicted by AHTpin and StackDPPIV, the top-scoring FCH peptides (ligands) depicted by the prediction software were used for molecular docking studies. The crystal structures of the human ACE receptor (PDB ID: 1O8A) and DPP-IV (PDB ID: 3KWF) were retrieved from the Protein Data Bank (https://www.rcsb.org/). The ACE and DPP-IV enzyme structure files were imported to the Discovery Studio Visualizer, where protein structures were prepared manually by removing all water molecules. However, the cofactors, zinc, and chloride were retained on the ACE receptor due to the catalytic function and influence on enzymatic activity. After the preparation of ligand and receptor molecules, AutoDock Vina with Lamarckian Genetic Algorithm was used for molecular docking [36]. The receptor and ligands were placed in a grid box of 40 × 40 × 40 xyz points with a spacing between points of 0.375 Å. The three-dimensional (3D) coordinates of the grid box were x = 40.57, y = 33.37, and z = 43.45 for ACE, and x = 18.44, y = 36.73, and z = 55.18 for DPP-IV. In addition, PyMOL 2.0 was used to visualise the 3D interactions of the ligand and the receptor protein. The standard inhibitors used were captopril and linagliptin for the ACE and DPP-IV enzymes, respectively [36, 37].

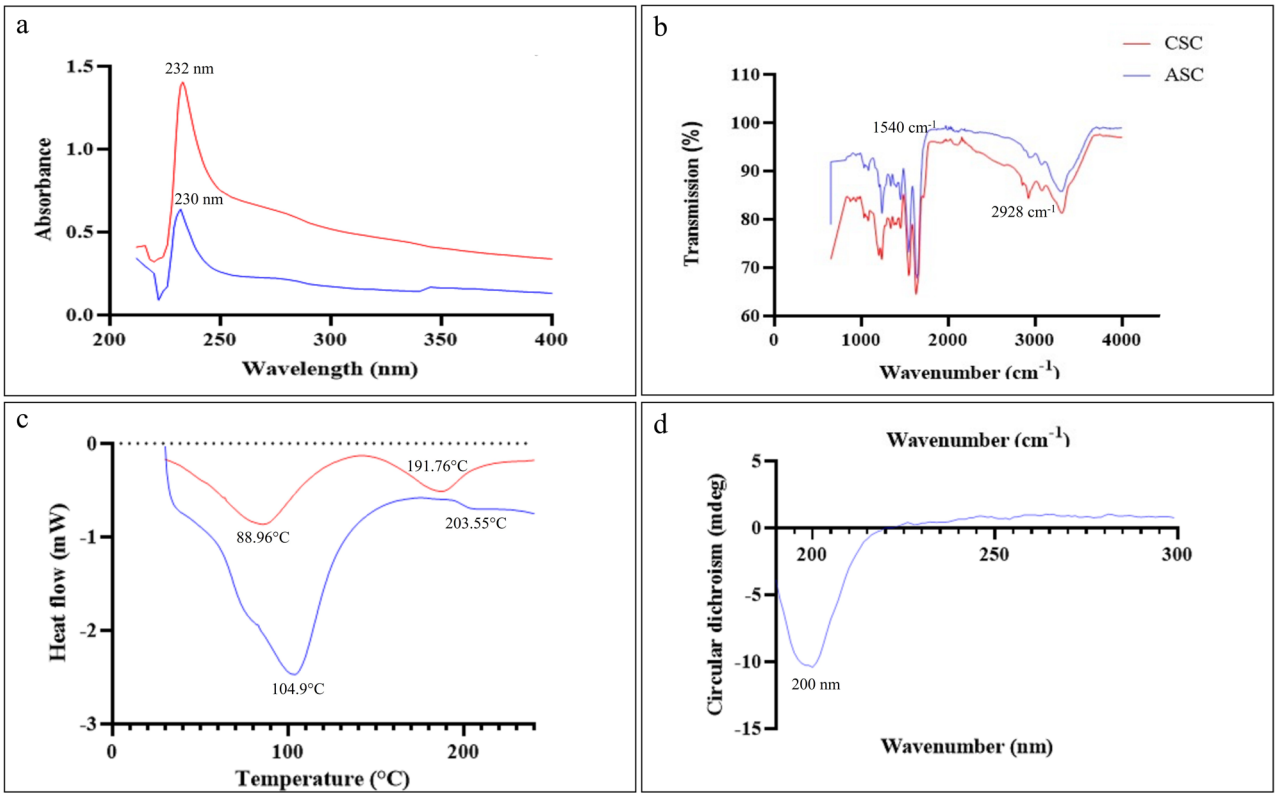

Fig. 1 Ultraviolet-visible spectroscopy (**a**), FT-IR spectroscopy (**b**), DCS (**c**), and CD spectroscopy (**d**) of the extracted ASC and CSC

2.7 Statistical analysis

Statistical analyses were performed using GraphPad Prism (version 10.4.2; GraphPad Software, Inc., San Diego, CA). In addition, comparisons between two groups were conducted using a two-tailed unpaired *t*-test with Welch's correction. All experiments were independently repeated at least three times, and data were presented as mean ± standard derivation (SD). A p-value < 0.05 was considered statistically significant.

3 Results and discussion

3.1 Biochemical and biophysical characterisation of ASC

The extraction yield of the ASC derived from the snapper salmon skin was 78.73 ± 8.51% (dry weight basis). The ASC extraction yield obtained in this study for fish skin was higher than the previously reported values by Ampitiya et al. [38] for yellowfin tuna (61.26% ± 0.63), seer fish (58.21% ± 0.27), and Asian sea bass (59.31% ± 2.87). The UV-Vis absorption spectrum for ASC between 210 and 400 nm displayed a maximum absorption peak for ASC at 232 nm (Fig. 1a), indicating the presence of tyrosine, tryptophan, and phenylalanine. The absorption effect can be attributed to the peptide bonds such as C=O, -COOH, and $CONH_2$, which were present in the triple helical polypeptide chain of the fish collagen. In addition, there was a slight absorption peak between 250 and 280 nm, indicating the low aromatic amino acid content such as tryptophan. Furthermore, the well-defined peaks in the ASC and CSC samples indicated the high purity of the collagen. These results also corroborated the *Centrolophus niger* skin collagen, in which a prominent peak was observed at 232 nm [2]. The FT-IR analysis of ASC revealed that the collagen structure consisted of hydrogen bonding with a carbonyl group in the peptide chain (Fig. 1b). The amide B bands of ASC (2928 cm^{-1}) indicated the asymmetrical stretching of CH_2, whereas the amide I band, with frequencies between 1600 and 1700 cm^{-1}, was characteristic of the stretching vibrations of the carbonyl group and the polypeptide backbone. The amide I band was present in the 1540 cm^{-1} range, confirming hydrogen bond formation between the N-H stretch in the X position and the C=O (glycine) of the fourth residue, which was responsible for the triple helix. The amide II and amide III bands represented the N-H bending vibrations in combination with the C-N stretching vibration and C-H stretching (Fig. 1b). Zhang et al. [39] also observed similar FT-IR patterns in the ASC extracted from waste Eel (*Anguilla japonica*) skin.

The DSC analysis depicted the thermal denaturation of ASC, which disrupted the triple helical structure, leading to the subsequent deterioration of the collagen structural characteristics. The thermal denaturation of both CSC and ASC was characterised by endothermic peaks at 88.96 °C and 104.91 °C, respectively. Further,

CSC and ASC depicted a second endothermic peak at 191.76 °C and 203.55 °C, respectively (Fig. 1c). The initial peak corresponds to the temperature at which the collagen and the water molecule bonds begin to denature. In contrast, the second endothermic peak signifies the differences in the structure of the cross-linked portion of collagen, ultimately resulting in its complete breakdown [24]. A study by Iswariya et al. [40] corroborated the current results, where a denaturation temperature of 78.9 °C for ASC was observed for the collagen derived from Pufferfish skin. Moreover, the CD spectra confirmed the triple-helical conformation of ASC with a negative peak at around 200 nm (Fig. 1d). In addition, Song et al. [41] reported that the maximum and minimum CD spectra for CSC were observed at 201 nm (negative absorption band). This characteristic peak is an indication of the triple helical collagen structure. Similarly, Zhang et al. [42] also reported an extremely negative peak at 200 nm for collagens extracted from Tilapia and Skate. Furthermore, the SDS-PAGE pattern depicted the characteristic alpha chains (α-1 and α-2) and a dimer (β chain), with α-1 having a double band intensity in the CSC and ASC lanes (Figure S1). The α chain directly relates to collagen primary structure and represents the interconnected components. Sousa et al. [43] also reported a similar SDS-PAGE pattern for the collagen derived from Atlantic cod. Subsequently, the amino acid profiling showed 311.67 glycine residues per 1000 amino acid residues (Table S1). Glycine has been reported to be the most abundant amino acid in the collagen chain and is present in every third residue in the central α-chain region, except for the N-terminus and C-terminus amino acid residues [1]. In addition, alanine, proline, and hydroxyproline were also observed to be in relatively high quantities, which are essential for the structural integrity of the collagen.

3.2 Composition and bioactivities of the collagen peptide fractions

The molecular weight distribution of the peptide fractions revealed distinct differences between the two hydrolysates (PTD and PDPTD). In PTD, peptides were predominantly present in the > 10 kDa fraction (51.20%), with comparatively lower yields in the < 3 kDa (11.83%) and 3–10 kDa (36.97%) ranges. In contrast, PDPTD showed a more balanced distribution, with a marked increase in the proportion of low-molecular-weight peptides (< 3 kDa, 33.30%), alongside comparable yields in

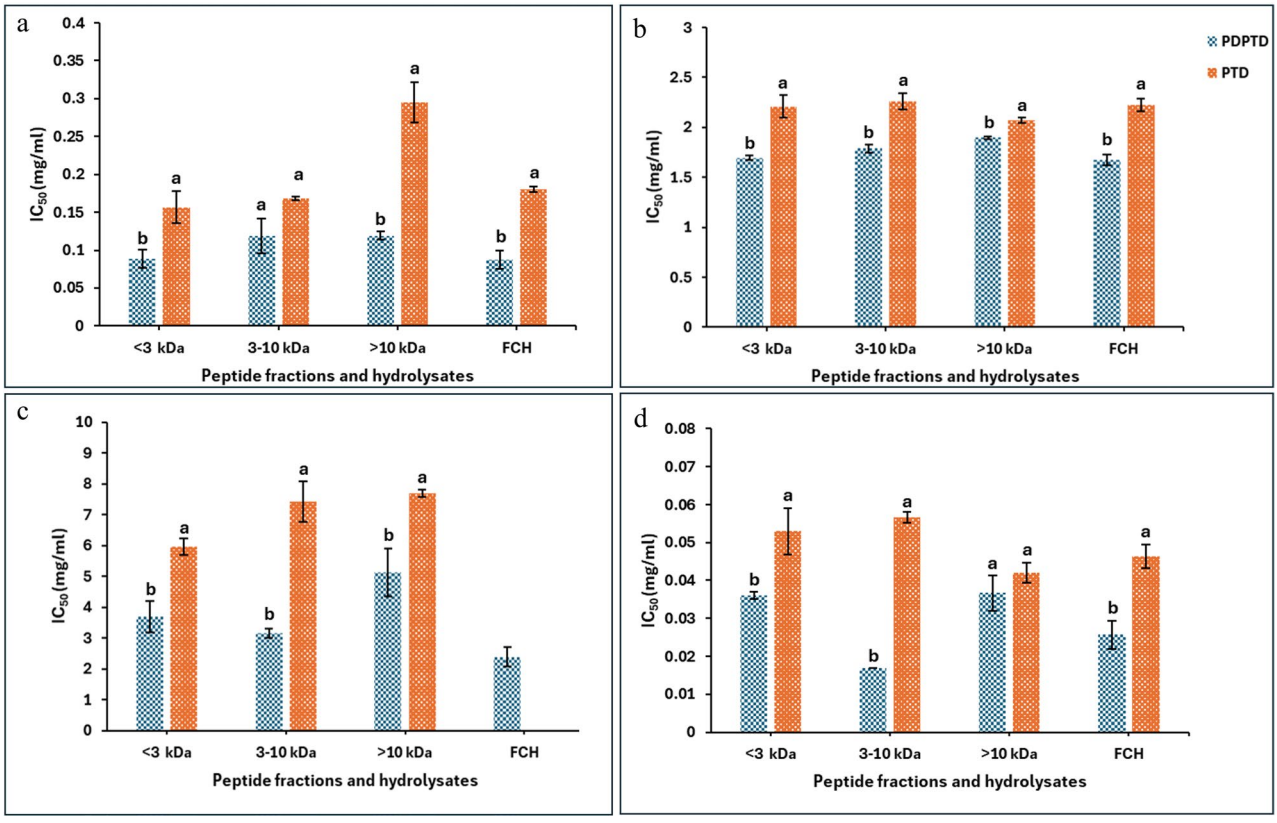

Fig. 2 Fig. 2 IC_{50} values of peptide fractions released during PDPTD and PTD for ACE (**a**), DPP-IV inhibitory (**b**), DPPH (**c**), and ABTS (**d**) activities. Data are presented as mean ± SD from three independent experiments (n=3). Statistical comparisons were performed using a two-tailed unpaired t-test with Welch's correction. Histograms sharing the same letter indicate no significant difference (p>0.05)

the 3–10 kDa (34.33%) and > 10 kDa (32.37%) fractions. This shift towards smaller peptides highlighted the efficiency of papain in promoting extensive protein hydrolysis, leading to the generation of low-molecular-weight peptides that are widely associated with improved bioavailability and enhanced biological activity. Accordingly, the bioactive potential of the different peptide fractions (< 3 kDa, 3–10 kDa, > 10 kDa and FCH) was subsequently evaluated through ACE inhibitory activity, DPP-IV inhibitory activity, and antioxidant activity assessed through DPPH and ABTS radical scavenging assays.

3.2.1 ACE inhibitory activity

Hypertension is a prevalent and significant chronic medical condition which poses a substantial risk for the onset of cardiovascular diseases. The ACE regulates blood pressure by converting angiotensin-I to angiotensin-II and deactivating bradykinin. The management of hypertensive conditions can be achieved using various drugs, including ACE inhibitors. The IC_{50} values of potential ACE inhibitory peptides derived from the FCH, as well as peptides released during PTD and PDPTD, were analysed (Fig. 2a). It was observed that the fish collagen peptides released during PDPTD depicted lower IC_{50} values than PTD, confirming more potent ACE inhibitory activity. In addition, the < 3 kDa fraction from PDPTD displayed a very low IC_{50} (0.089 ± 0.01 mg/mL), suggesting that low-molecular-weight peptide fractions may inhibit the ACE enzyme more efficiently than high-molecular-weight fractions. Similarly, the peptides released during PTD also displayed a similar phenomenon. Overall, for PDPTD, the FCH showed significant ACE inhibitory activity with an IC_{50} of 0.088 ± 0.01 mg/mL. The findings indicated that the ACE inhibitory activity is dose-dependent. Furthermore, Ishak et al. [44] reported an IC_{50} of 2.20 mg/mL for the < 3 kDa peptide fraction, which was derived from the Shortfin scad (*Decapterus macrosoma*) protein hydrolysate. The result obtained was higher than the IC_{50} for the < 3 kDa peptide fraction in the current study, hence lower inhibitory activity. ACE inhibitory activity has also been reported for Nile tilapia collagen hydrolysates by Thuanthong et al. [45] with an IC_{50} value of 1.2 mg/mL, which is also higher than the ACE inhibitory activity of the FCH derived from the current study.

3.2.2 DPP-IV inhibitory activity

DPP-IV functions as a dipeptidase, playing a role in breaking down the incretin hormones, specifically glucagon-like peptide-1 (GLP-1) and glucose-dependent insulinotropic peptide (GIP). These incretins are essential in regulating insulin secretion and, consequently, glycaemic control. DPP-IV inhibition results in extending the half-life of GLP-1 and GIP, leading to augmented insulin production. The current study observed that the peptides released during PDPTD had the lowest IC_{50} and hence displayed the highest DPP-IV inhibitory activity compared to peptides released by PTD (Fig. 2b). FCH released during PDPTD had an IC_{50} of 1.67 ± 0.06 mg/mL; however, during PTD, FCH exhibited a half-maximal inhibition of 2.22 ± 0.07 mg/mL. Furthermore, the current study depicted higher DPP-IV inhibitory activity compared to that reported by Cao et al. [10], who reported an IC_{50} of 5.45 ± 0.24 mg/mL derived from Eel protein hydrolysates. Additionally, Guo et al. [46] reported that following simulated gastrointestinal digestion, the DPP-IV potency of the Alaska pollock skin collagen exhibited 2.59 ± 0.04 mg/mL which was higher than the IC_{50} exhibited by the FCH in this study. Furthermore, the < 3 kDa fraction released during PDPTD possessed a very low IC_{50} of 1.69 ± 0.02 mg/mL, confirming effective DPP-IV inhibitory potential. In relation, Cheung and Li-Chan [11] also reported that low-molecular-weight (< 3 kDa) peptides derived from the protein hydrolysates of Steelhead (*Oncorhynchus mykiss*) exhibited the highest DPP-IV inhibitory activity. Hence, the peptide fractions and FCH released during PDPTD could be superior DPP–IV inhibitors.

3.2.3 DPPH radical scavenging activity

The antioxidant activity of any substance can be estimated by its effectiveness in stabilising and scavenging the DPPH radicals [47]. In this regard, neutralising the stable DPPH radical is commonly employed for analysing the free radical scavenging capability of various samples including bioactive peptides. All the peptide fractions including the FCH released by PDPTD, displayed lower IC_{50} values than PTD (Fig. 2c). In other words, when fish collagen was predigested with papain before PTD, it demonstrated a higher efficiency in neutralising DPPH free radicals. The FCH released during PDPTD exhibited an IC_{50} of 2.38 ± 0.31 mg/mL; however, the FCH from PTD displayed DPPH scavenging activity only at higher tested concentrations, indicating significantly higher IC_{50} values beyond the experimental range. The IC_{50} of the FCH was similar to the salmon protein hydrolysates reported by Ahn et al. [48], where IC_{50} values of 4.76 ± 0.22, 4.95 ± 0.31, 4.53 ± 0.24 mg/mL were recorded subsequent to alcalase, neutrase, and trypsin hydrolysis, respectively. The IC_{50} for FCH was also significantly lower than the IC_{50} of the Blue shark skin gelatine hydrolysates which was 13.0 mg/mL [49]. Nurilmala et al. [12] also reported that the 3–10 kDa peptide fractions derived from Yellowfin tuna exhibited the highest DPPH scavenging activity. The study was consistent with Nurdiani et al. [50], who reported high antioxidant (DPPH) activity for peptides (3–10 kDa) derived from flathead byproducts. It was also observed that mostly low-molecular-weight peptides showed the highest antioxidant activity

Table 1 In silico analysis of the bioactivity potential of top peptide candidates derived from FCH released by PTD

Peptide sequence/ PeptideRanker (FRS score)	ACE inhibitory activity		DPP-IV inhibitory activity		Physicochemical properties					Binding affinity (kcal/mol)	
	Score	Prediction	Score	Prediction	Molecular weight (g/mol)	Extinction coefficient (1/M·cm)	Isoelectric point (pI)	Net charge	Water solubility	ACE	DPP-IV
AGPPGPPGPS 0.84 (0.59)	0.92	AHT	0.85	DPP-IV	832.9	0	3.79	0	Poor	-10.1	-8.5
APGFQGLP 0.88 (0.48)	1.3	AHT	0.77	DPP-IV	785.89	0	3.88	0	Poor	-10.8	-6.9
GEHGPPGPA 0.57 (0.59)	1.47	AHT	0.41	non-DPP-IV	817.85	0	5.1	-0.9	Good	19.7	-9.2
GPPGEPGPLG 0.9 (0.56)	0.42	AHT	0.95	DPP-IV	876.95	0	0.9	-1	Good	-19.6	-9.8
PGPPGPPSF 0.95 (0.57)	0.77	AHT	0.93	DPP-IV	851.94	0	4.15	0	Poor	-10	-9.2

*ND – Not detected

Table 2 In silico analysis of the bioactivity potential of top peptide candidates derived from FCH released by PDPTD

Peptide sequence/ PeptideRanker (FRS score)	ACE-inhibitory activity		DPP-IV inhibitory activity		Physicochemical properties					Binding affinity (kcal/mol)	
	Score	Prediction	Score	Prediction	Molecular weight (g/mol)	Extinction coefficient (1/M·cm)	Isoelectric point (pI)	Net charge	Water solubility	ACE	DPP-IV
GPAGPHGPPGK 0.89 (0.61)	1.05	AHT	0.48	non-DPP-IV	971	0	10.1	1.1	Good	-11	-8.2
GPSGPPGPPGS 0.87 (0.57)	0.53	AHT	0.87	DPP-IV	906	0	3.72	0	Good	-10.4	-9
GSAGPPGPPGP-PGPPG 0.92 (0.68)	1.08	AHT	0.81	DPP-IV	1295	0	3.62	0	Poor	-11.3	-8.8
IGFPGFPG 0.93 (0.51)	0.67	AHT	0.81	DPP-IV	791	0	3.63	0	Poor	-11.2	-9.1
PDGPPGPM 0.93 (0.56)	0.43	AHT	0.85	DPP-IV	767	0	0.78	-1	Good	-0.8	-9.4

*ND – Not detected

due to the presence of specific amino acids. For instance, alanine, glycine, or glutamic acid are mostly exposed, leading to increased interactions between peptides and lipid substances, consequently enhancing the stability of free radicals [51]. Antioxidant activity can also be influenced by the presence of hydrophobic amino acids[52]. On the contrary, the intact collagen did not show any DPPH scavenging activity. This suggested that antioxidant peptides remained inactive within the sequences of their parent protein but were released during enzymatic hydrolysis [53, 54]. The results indicated that the peptide fractions released during PDPTD exhibited higher DPPH radical scavenging activity, suggesting a greater potential to convert DPPH radicals into less harmful substances as compared to the peptides released by PTD.

3.2.4 ABTS radical scavenging activity

The ABTS assay involves the oxidation of ABTS by potassium persulfate, generating a blue-green $ABTS^{\bullet+}$ radical cation, which has a peak absorption at 734 nm. The peptides released during PDPTD depicted the lowest IC_{50} and, therefore, the highest ABTS scavenging activity (Fig. 2d). The peptide fraction (3–10 kDa) displayed the lowest IC_{50} value of 0.017 ± 0.00 mg/mL. The increase in ABTS activity could be attributed to specific amino acids in the peptide chain, notably tyrosine and phenylalanine [55]. Besides these amino acids, glutamine, asparagine, glycine, and aspartate may augment antioxidant activity by providing surplus electrons to neutralise free radicals [52]. Similarly, Park and Jo [3] reported that low-molecular-weight peptide fractions have the highest antioxidant activity from collagen extracted from fish byproducts. The FCH released during PDPTD depicted an IC_{50} value of 0.026 ± 0.004 mg/mL, whereas FCH released during

PTD had an IC_{50} value of 0.046 ± 0.003 mg/mL. Therefore, the peptides released during PDPTD demonstrated the ability to neutralise ABTS radicals, effectively halting the radical chain reaction and thereby preventing lipid oxidation through a chain-breaking mechanism. All these results corroborated the significant contribution of the pre-digestion of collagen with papain before in vitro pepsin-trypsin digestion, where peptides generated from PDPTD had significantly lower IC_{50} values than those generated by PTD. The significantly lower bioactivities observed in this study could be attributed to digestion, as this is the first study to report collagen protein digestion with papain first, followed by pepsin-trypsin digestion, whereas previous studies only tested the effect of individual enzymes.

3.3 Identification of potential bioactive peptides from FCH

LC-MS/MS analysis was used to identify the peptide sequences in the FCH derived from PDPTD and PTD. The FCH was selected since the hydrolysates displayed comparable antioxidant, ACE and DPP-IV inhibitory activities to the peptide fractions. Results showed that the FCH of PTD contained 25 unique peptide sequences out of a total of 47 detected, while the FCH of PDPTD contained 54 unique sequences out of 116 detected (Tables 1 and 2, Tables S2 and S3). It was observed that the number of peptides released was higher in PDPTD than in PTD, which can be attributed to the number of additional enzymes used during PDPTD. In addition, it can also be noted that a higher number of released peptides increases the likelihood of enhanced bioactive properties. Therefore, the identification of the peptides prompted additional in silico analyses to better understand their physicochemical properties and potential bioactivities that may be exhibited solely by the peptides.

3.4 PeptideRanker analysis of BPs

The peptides identified from the FCH released after PDPTD in vitro using LC-MS/MS analysis were further screened using PeptideRanker (Tables 1 and 2, Tables S2 and S3). For example, the top-ranked peptides released during PDPTD were IGFPGFPG, PDGPPGPM, PQGYPGIGKPGMPGMP, and GPPGPMGPPGLPGLK with scores of 0.93, 0.93, 0.93, and 0.96, respectively. Similarly, during PTD, GPAGPPGNPGPPGPPGP, PDGPPGPM, GPPGPPGPAG, and PGPPGPPSF depicted scores of 0.93, 0.93, 0.94, and 0.95, respectively. The peptides with scores greater than 0.5 were considered potential BPs; however, if less than 0.5, they were not regarded as bioactive [36]. In addition, most peptides that depicted potential bioactivity had glycine and proline in abundance, as they are known to serve as potential precursors for BPs [23]. This type of analysis draws its conclusion based on the structure-function analysis by evaluating how the peptide structure influences the biological activity exhibited. Liu et al. [31] reported 24 peptides from Yak bone collagen, which were potentially bioactive. These results also corroborated the PeptideRanker analysis for the fish collagen, in which 25 and 54 peptides were also derived from PTD and PDPTD, respectively. PeptideRanker does not test for specific bioactivity; however, it provides an overall prediction of the probability that a specific peptide sequence will exhibit any biological activity. Therefore, these BPs were further screened for their specific bioactivities using AnOxPePred, AHTpin, and StackDPPIV software.

3.5 Potential bioactivities exhibited by FCH after PDPTD and PTD

The potential antioxidant activity of the peptides was analysed using the AnOxPePred software. In other words, the higher the score is, the more likely the peptides are to have free radical scavenging activity. For example, PTD action showed the release of peptide GPAGPPGNPGPPGPPGP (0.63), with good free radical scavenging (FRS) potential, whereas PDPTD treatment showed the release of peptide GSAGPPGPPGPPGPPG (0.68), with a better FRS potential (Tables 1 and 2, Tables S2 and S3). Subsequently, the AHTpin software was also used to analyse the potential ACE inhibitory activity exhibited by the peptides. For instance, PTD released 24 potential ACE inhibitory peptides and 21 potential DPP-IV inhibitory peptides, while PDPTD released 48 and 20, respectively. The peptides released after PTD and PDPTD were abundant in amino acids, glycine and proline. The amino acids possibly influenced the potential bioactivities they exhibited. For instance, Ayati et al. [7] suggested that the DPP-IV inhibitory activity of peptides derived from fish collagen can be significantly influenced by amino acids, including phenylalanine, proline, leucine, isoleucine, and glycine, because they promote hydrophobic interactions with the DPP-IV active site. Furthermore, the pyrrole ring found in proline is crucial in inhibiting ACE and helps peptides digest more steadily in the gastrointestinal tract [4]. The potentially BPs were then subjected to physicochemical property analysis to further understand how these properties enhance the efficiency of these peptides.

3.6 Physicochemical properties

Physicochemical properties provide an overall understanding of the peptide sequences, which is essential for optimising the mechanisms to further comprehend the applications of the potential BPs derived from PeptideRanker. The in silico platform, PepCalc, was utilised to determine molecular properties such as molecular weights, pI, and extinction coefficients of the peptides released by the FCH after PTD and PDPTD (Tables 1

and 2, Tables S2 and S3). For PTD, the molecular weight observed ranged from 0.76 to 1.41 kDa, whereas 0.76 to 2.26 kDa was observed for PDPTD. Similarly, Wardani et al. [56] also reported molecular wight ranging from 0.26 to 1.45 kDa of peptides derived from yellowfin skin tuna collagen. It was observed that the range of molecular wight exhibited greater antioxidant activity. The current study indicates that most of the ACE and DPP-IV inhibitory peptides have a low-molecular-weight profile. In addition, the in vitro results mostly showed that low-molecular-weight peptides exhibited better bioactivity than high-molecular-weight peptides, aligning with the physicochemical properties. Pal and Suresh [23] also reported that peptides with low-molecular-weight had good antioxidant activity. The net charge of a peptide indicates the balance between its positively and negatively charged amino acids, determining whether a peptide is overall positively charged, negatively charged, or neutral. Auwal et al. [57] suggested that peptides with pI in the acidic and basic points depicted higher ACE inhibitory activity than those separated at neutral points. For instance, for PTD, the pI ranged from 0.68 to 10.84; similarly, for PDPTD, the pI ranged from 0.62 to 10.9. In addition, Munawaroh et al. [58] reported that the charges of peptide sequences can reveal the relationship between receptor binding affinity and ionic interactions, which can be further explored through molecular docking analyses. Additionally, the molar extinction coefficient measures how much light a peptide absorbs at a certain wavelength, generally 280 nm for proteins. When a chromophore is present, such as tryptophan or tyrosine, the molar extinction coefficient becomes an important tool for assessing the peptide content [59]. For example, HSLPHYLG and PQGYPGIGKPGMPGMP were the only two sequences derived from PDPTD, which depicted an extinction coefficient of 1280 M^{-1} cm^{-1} due to tyrosine. However, peptides derived from PTD did not display an extinction coefficient. In addition, tyrosine and tryptophan are frequently targets for enzymatic alteration, such as phosphorylation or oxidation, which can result in deterioration or altered function [60]. Therefore, since the peptides did not constitute these residues, they might have the potential to be resistant to peptide modifications and, ultimately, enzymatic digestion. Overall, the physicochemical features of peptide sequences determined their potential bioactivity, and molecular docking was then used to investigate the impact of these properties on peptide sequences and their inhibitory actions.

3.7 Molecular docking studies

Molecular docking is a widely employed approach for exploring the interaction dynamics between molecules, predicting their binding patterns, and estimating their binding strength. The peptides displaying potential ACE and DPP-IV inhibitory activity after screening with the predictive software AHTpin and StackDPPIV were further analysed using molecular docking for confirmatory purposes. The molecular interactions between the enzymes and peptides included conventional hydrogen bonds, carbon-hydrogen bonds, pi-cation, pi-pi T-shaped, alkyl and pi-alkyl bonds, which further played a significant role corresponding to the described bioactivities (Figs. 3 and 4, Figure S2 and S3). Additionally, the energy interactions are stable when the binding affinity

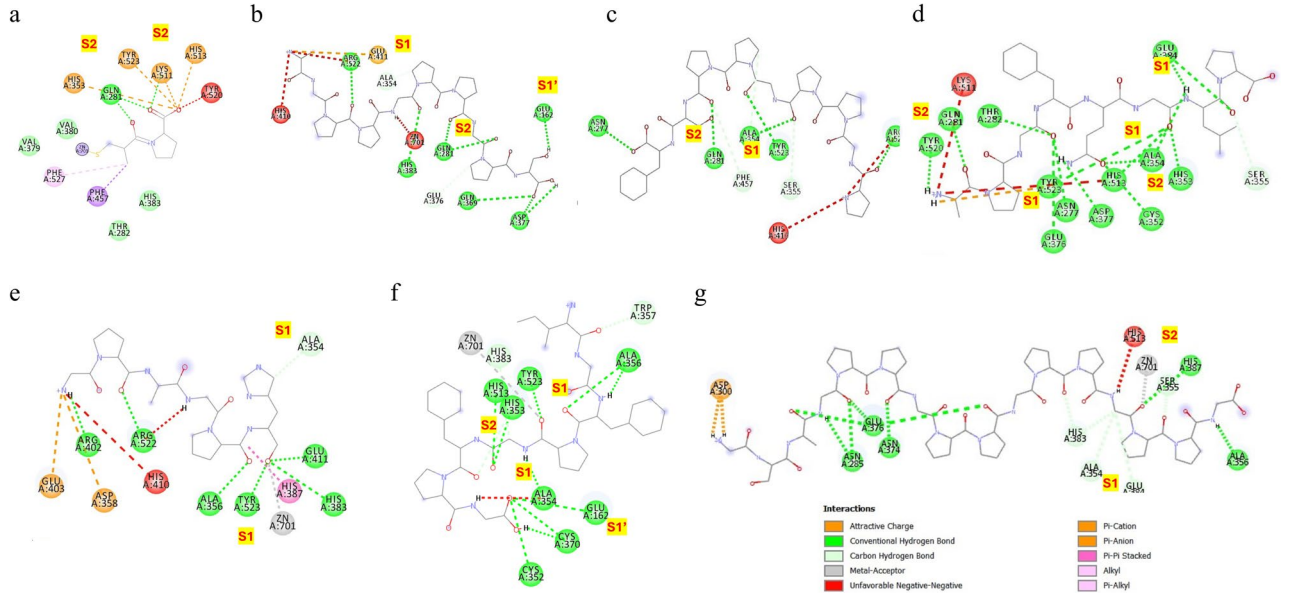

Fig. 3 2D diagrams of docked poses and interactions of ACE receptor with standard inhibitor captopril (**a**), and peptides AGPPGPPGPS (**b**), PGPPGPPSF (**c**), and APGFQGLP (**d**) released after PTD; and peptides GPAGPHGPPGK (**e**), IGFPGFPG (**f**), and GSAGPPGPPGPPGPPG (**g**) released after PDPTD

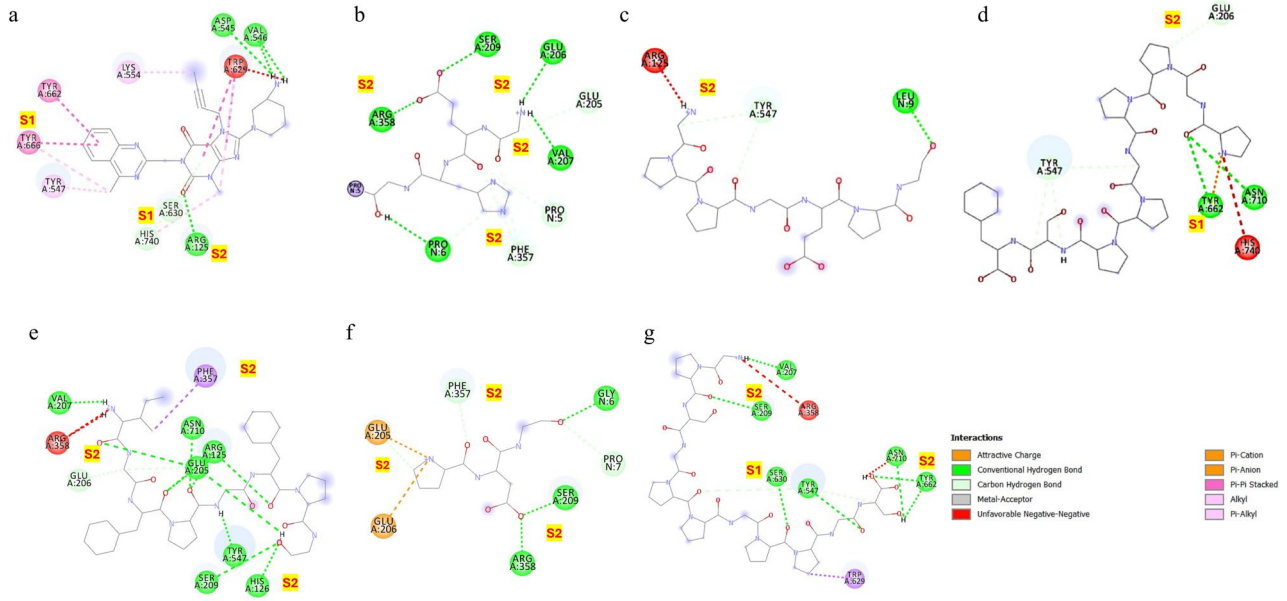

Fig. 4 2D diagrams of docked poses and interactions of DPP-IV receptor with standard inhibitor linagliptin (**a**) and peptides GEHGPPGPA (**b**), GPPGEPGPLG (**c**), PGPPGPPSF (**d**) released after PTD; and IGFPGFPG (**e**), PDGPPGPM (**f**), and GPSGPPGPPGS (**g**) released after PDPTD

between the target protein and ligand ranges from –5 to -15 kcal/mol [61]. A more negative score meant that the peptide (ligand) was more likely to bind strongly to the protein (target), thus facilitating more favourable interactions [62]. For the ACE enzyme, the binding energy of the standard inhibitor captopril (-5.6 kcal/mol) was higher than that of the peptides evaluated in this study. This was an indication that the selected peptides derived from PTD and PDPTD displayed promising ACE activity. The main interacting residues at the ACE active site are separated into three pockets (S1, S2 and S1′). The S1 pocket comprises alanine354, glutamic acid384, and tyrosine523 residues; S2 pocket includes glutamine281, histidine353, lysine511, histidine513, and tyrosine520 residues; while S1′ is made up of glutamic acid162 residues [63]. In addition, the cofactor Zn (II) at the ACE active site also plays a critical role and is bound to ACE residues of histidine383, histidine387, and glutamic acid411. It was observed that inhibitors with binding affinity towards these pockets or zinc tetrahedral coordination might have a high inhibitory capacity for the ACE enzyme [64]. Similarly, Li et al. [65] also reported the significance of Zn in naked oat bran albumin hydrolysates and the efficiency in zinc chelating activity and ACE inhibitory activity.

In the current study, the top three peptides, APGFQGLP, AGPPGPPGPS, and PGPPGPPSF, released after PTD displayed the lowest binding energies of -10.8, -10.1 and -10 kcal/mol, respectively. Furthermore, APGFQGLP (-10.8) kcal/mol interacted with amino acids such as alanine354, glutamic acid384, tyrosine523, glutamine281, histidine353, histidine513, tyrosine520, and depicted conventional hydrogen bonds. Additionally, the peptide sequences, GSAGPPGPPGPPGPP (-11.3 kcal/mol), IGFPGFPG (-11.2 kcal/mol), GPAGPHGPPGK (-10.4 kcal/mol), released after PDPTD, displayed comparatively better binding energies than the peptides released after PTD. It was also observed that there were no interactions between the zinc ion and the peptides released after PTD. These peptides (PDPTD) interact with the ACE enzyme by mostly conventional hydrogen bonds and with the zinc ion, hence improving the ACE inhibitory ability of the peptides. In addition, hydrogen bonding also improves the stability between the peptide-ligand complex and the ACE enzyme [58].

Besides ACE inhibition, the need for peptides, which can depict DPP-IV inhibitory activity to combat type-2 diabetes is also essential. DPP-IV comprises a concave-shaped active site and potential inhibitors frequently engage in competitive binding within this active site by targeting subsites S1 and/or S2 nestled within the cavity. The hydrophobic S1 subsite consists of the catalytic triad serine630-aspartate708-histidine740 along with hydrophobic amino acids (tyrosine631, tryptophan659, tyrosine662, tyrosine666, valine711, and valine656). The charged S2 subsite comprises glutamic acid205, glutamic acid206, arginine125, serine209, arginine358, valine207, and phenylalanine357 [58]. The present study depicted the interacting residues of DPP-IV with linagliptin (standard inhibitor), which were histidine740, tyrosine662, tyrosine666, arginine125, and serine630. The peptides GPPGEPGPLG (-9.8 kcal/mol), PGPPGPPS (-9.2 kcal/mol), and GEHGPPGPA (-9.2 kcal/mol) released after PTD, as well as PDGPPGPM (-9.4 kcal/mol), IGFPGFPG (-9.1 kcal/mol), and GPSGPPGPPGS (-9.0 kcal/

mol) released after PDPTD depicted the strong binding energies to the DPP-IV enzyme. Like the ACE enzyme, hydrogen bonds were predominant between the peptides and amino acid residues at the active site of the DPP-IV enzyme. The peptides which showed potential inhibitory activity were mostly composed of glycine and proline. In this context, Xu et al. [66] reported that glycine-proline-type peptides enhanced the affinity to DPP-IV when interacting with the protein's S2, S2′ subsites. Moreover, it was observed that the peptide sequence IGFPGFPG released after PDPTD was the only peptide to bind with both the ACE and DPP-IV and to depict comparatively lower binding energies. Furthermore, IGFPGFPG's suitability for ACE inhibition was reinforced by strong binding energy, zinc coordination, and the presence of multiple hydrogen bonds, all of which enhanced its interactions with the enzyme. The strong bioactivity of IGFPGFPG can be attributed to its structural features. Its high content of hydrophobic amino acids, such as isoleucine, phenylalanine, and proline promotes interactions with hydrophobic pockets of ACE and DPP-IV. Aromatic residues like phenylalanine also contribute to antioxidant activity through electron donation and radical stabilisation. The presence of IGFPGFPG among the PDPTD-released peptides likely contributed to the enhanced bioactivities of the FCH. The study highlighted the peptides' potential to act as suitable inhibitory peptides and exhibit potential bioactivity towards ACE and DPP-IV.

4 Conclusion

This study demonstrated that using papain as a pre-digestive enzyme for releasing collagen peptides from fish waste enhanced their potential ACE inhibitory, DPP-IV inhibitory, and antioxidant activities. These peptides possessed various bioactive properties that could be considered a cost-effective and health-promoting alternative to synthetic ones. In addition, the FCH from PDPTD exhibited lower IC_{50} values of 0.088 ± 0.01 mg/mL (ACE), 1.67 ± 0.06 mg/mL (DPP-IV), 2.38 ± 0.31 mg/mL (DPPH), and 0.026 ± 0.004 mg/mL (ABTS), which were comparable to the low-molecular-weight fractions. This is an indication that the peptides released during PDPTD demonstrated improved ACE inhibitory, DPP-IV inhibitory, and antioxidant activity compared to PTD. It was observed that the FCH displayed comparable activity to the low-molecular-weight peptide fractions, making it a suitable source of BPs and reducing purification costs. It is important to note that utilising papain as a pre-digestive enzyme exhibited significant bioactive properties compared to in vitro pepsin-trypsin digestion of collagen. The study also confirmed that the peptide IGFPGFPG, released from PDPTD, depicted relatively high binding energies to the ACE and DPP-IV enzymes, which demonstrated the peptide's significant inhibitory activity and multifunctional bio-efficacy, thereby highlighting its potential as a candidate for further development in therapeutic applications targeting hypertension, diabetes, and oxidative stress-related disorders. However, further studies should be conducted to explore the potential of synthesised peptides and their bioactivities. The study concluded that fish waste can serve as a valuable source of BPs, whose bioactive potential can be enhanced by pre-digesting it with the papain enzyme.

Supplementary Information

The online version contains supplementary material available at https://doi.org/10.1186/s42825-026-00248-7.

Supplementary Material 1.

Acknowledgements
The authors would like to thank Prof. John Mellem for his valuable assistance with the Varioskan Lux Multimode Microplate Reader.

Author contributions
PB and SP contributed to the study conception and design. Material preparation, data collection and analysis were performed by CE and PB. The first draft of the manuscript was written by CE and all authors commented on previous versions of the manuscript. All authors read and approved the final manuscript.

Funding
This work was supported by the National Research Foundation of South Africa under grant numbers [MND 210510600423, RA22111973672, RA210116582014 and CPRR240509218140] and Innovation Builder Funding, Durban University of Technology, South Africa.

Data availability
The data and materials that support the findings of this study are available from the corresponding author upon reasonable request.

Declarations

Ethics approval and consent to participate
Not applicable.

Consent for publication
Not applicable.

Competing interests
The authors declare that they have no known competing financial interests or personal relationships that could have appeared to influence the work reported in this paper.

Author details
[1]Department of Biotechnology and Food Science, Faculty of Applied Sciences, Durban University of Technology, P.O. Box 1334, Durban 4000, South Africa
[2]Department of Polymer Chemistry and Technology, Kaunas University of Technology, Radvilenu Rd. 19, 50254 Kaunas, Lithuania

Received: 9 October 2025 / Revised: 13 February 2026 / Accepted: 23 February 2026
Published online: 15 April 2026

References

1. Zhao C, Xiao Y, Ling S, Pei Y, Ren J. Structure of collagen. Fibrous Proteins: Design, Synthesis, and Assembly; 2021. pp. 17–25.

2. Bhuimbar MV, Bhagwat PK, Dandge PB. Extraction and characterization of acid soluble collagen from fish waste: development of collagen-chitosan blend as food packaging film. J Environ Chem Eng. 2019;7(2):102983.
3. Park SH, Jo Y-J. Static hydrothermal processing and fractionation for production of a collagen peptide with anti-oxidative and anti-aging properties. Process Biochem. 2019;83:176–82. https://doi.org/10.1016/j.procbio.2019.05.015.
4. Dong Y, Yan W, Zhang Y-Q, Dai Z-Y. A novel angiotensin-converting enzyme (ACE) inhibitory peptide from tilapia skin: preparation, identification and its potential antihypertensive mechanism. Food Chem. 2024;430:137074. . https://doi.org/10.1016/j.foodchem.2023.137074
5. Bhagwat P, Dandge P. Collagen and collagenolytic proteases: a review. Biocatal Agric Biotechnol. 2018;15:43–55. . https://doi.org/https://doi.org/. https://doi.org/10.1016/j.bcab.2018.05.005
6. Xu N, Peng X-L, Li H-R, Liu J-X, Cheng J-S-Y, Qi X-Y, Ye S-J, Gong H-L, Zhao X-H, Yu J. Marine-derived collagen as biomaterials for human health. Front Nutr. 2021;8:702108.
7. Ayati S, Eun J-B, Atoub N, Mirzapour-Kouhdasht A. Functional yogurt fortified with fish collagen-derived bioactive peptides: antioxidant capacity, ACE and DPP-IV inhibitory. J Food Process Preserv. 2022;46(1):e16208. . https://doi.org/10.1111/jfpp.16208
8. Coppola D, Lauritano C, Palma Esposito F, Riccio G, Rizzo C, de Pascale D. Fish Waste: from problem to valuable resource. Mar Drugs. 2021;19(2). https://doi.org/10.3390/md19020116
9. Caruso G, Floris R, Serangeli C, Di Paola L. Fishery wastes as a yet undiscovered treasure from the sea: biomolecules sources, extraction methods and valorization. Mar Drugs. 2020;18(12):622.
10. Cao H, Di N, Jiang B, Chen J, Zhang T. Purification and characterization of the dipeptidyl peptidase-IV inhibitory peptides from eel (Anguilla rostrata) scraps enzymatic hydrolysate for the treatment of type 2 diabetes mellitus. J Sci Food Agric. 2023;103(7):3714–24. https://doi.org/10.1002/jsfa.12462.
11. Cheung IWY, Li-Chan ECY. Enzymatic production of protein hydrolysates from steelhead (Oncorhynchus mykiss) skin gelatin as inhibitors of dipeptidyl-peptidase IV and angiotensin-I converting enzyme. J Funct Foods. 2017;28:254–64. https://doi.org/10.1016/j.jff.2016.10.030.
12. Nurilmala M, Hizbullah HH, Karnia E, Kusumaningtyas E, Ochiai Y. (2020) Characterization and antioxidant activity of collagen, gelatin, and the derived peptides from Yellowfin Tuna (Thunnus albacares) skin. Marine Drugs, 18(2), 98. https://www.mdpi.com/1660-3397/18/2/98
13. Cruz-Casas DE, Ramos-González R, Prado-Barragán LA, Iliná A, Aguilar CN, Rodríguez-Herrera R, Tsopmo A, Flores-Gallegos AC. Protein hydrolysates with ACE-I inhibitory activity from amaranth seeds fermented with Enterococcus faecium-LR9: identification of peptides and molecular docking. Food Chem. 2025;464:141598. . https://doi.org/10.1016/j.foodchem.2024.141598
14. Abuine R, Rathnayake AU, Byun H-G. Biological activity of peptides purified from fish skin hydrolysates. Fisheries Aquat Sci. 2019;22(1):1–14.
15. Hema G, Joshy C, Shyni K, Chatterjee NS, Ninan G, Mathew S. Optimization of process parameters for the production of collagen peptides from fish skin (Epinephelus malabaricus) using response surface methodology and its characterization. J Food Sci Technol. 2017;54:488–96.
16. Ritian J, Teng X, Liao M, Zhang L, Wei Z, Meng R, Liu N. Release of dipeptidyl peptidase IV inhibitory peptides from salmon (Salmo salar) skin collagen based on digestion–intestinal absorption in vitro. Int J Food Sci Technol. 2021;56(7):3507–18. https://doi.org/10.1111/ijfs.14977.
17. Xiong Z, Cheng J, Hu Y, Chen S, Qiu Y, Yang A, Wu Z, Li X, Chen H. A composite enzyme derived from papain and chymotrypsin reduces the allergenicity of cow's milk allergen casein by targeting T and B cell epitopes. Food Chem. 2024;459:140315.
18. Elisha C, Bhagwat P, Pillai S. Emerging production techniques and potential health promoting properties of plant and animal protein-derived bioactive peptides. Crit Rev Food Sci Nutr. 2025;65(24):4729–58. https://doi.org/10.1080/10408398.2024.2396067.
19. Rehm FB, Jackson MA, De Geyter E, Yap K, Gilding EK, Durek T, Craik DJ. Papain-like cysteine proteases prepare plant cyclic peptide precursors for cyclization. Proc Natl Acad Sci. 2019;116(16):7831–6.
20. Choudhary R, Kaushik R, Chawla P, Manna S. Exploring the extraction, functional properties, and industrial applications of papain from Carica papaya. J Sci Food Agric. 2025;105(3):1533–45. https://doi.org/10.1002/jsfa.13776.
21. Tacias-Pascacio VG, Castañeda-Valbuena D, Morellon-Sterling R, Tavano O, Berenguer-Murcia Á, Vela-Gutiérrez G, Rather IA, Fernandez-Lafuente R. Bioactive peptides from fisheries residues: a review of use of papain in proteolysis reactions. Int J Biol Macromol. 2021;184:415–28. . https://doi.org/10.1016/j.ijbiomac.2021.06.076
22. Faralizadeh S, Rahimabadi EZ, Bahrami SH, Hasannia S. Extraction, characterization and biocompatibility evaluation of silver carp (Hypophthalmichthys molitrix) skin collagen. Sustainable Chem Pharm. 2021;22:100454. https://doi.org/10.1016/j.scp.2021.100454.
23. Pal GK, Suresh PV. Physico-chemical characteristics and fibril-forming capacity of carp swim bladder collagens and exploration of their potential bioactive peptides by in silico approaches. Int J Biol Macromol. 2017;101:304–13. https://doi.org/10.1016/j.ijbiomac.2017.03.061.
24. Gauza-Włodarczyk M, Kubisz L, Mielcarek S, Włodarczyk D. Comparison of thermal properties of fish collagen and bovine collagen in the temperature range 298–670K. Mater Sci Engineering: C. 2017;80:468–71. https://doi.org/10.1016/j.msec.2017.06.012.
25. Laemmli UK. Cleavage of structural proteins during the assembly of the head of bacteriophage T4. Nature. 1970;227(5259):680–5.
26. Kulkarni P, Maniyar M, Nalawade M, Bhagwat P, Pillai S. Isolation, biochemical characterization, and development of a biodegradable antimicrobial film from Cirrhinus mrigala scale collagen. Environ Sci Pollut Res. 2022;29(13):18840–50. https://doi.org/10.1007/s11356-021-17108-y.
27. Liao W, Chen H, Jin W, Yang Z, Cao Y, Miao J. Three newly isolated calcium-chelating peptides from tilapia bone collagen hydrolysate enhance calcium absorption activity in intestinal Caco-2 cells. J Agric Food Chem. 2020;68(7):2091–8.
28. Re R, Pellegrini N, Proteggente A, Pannala A, Yang M, Rice-Evans C. Antioxidant activity applying an improved ABTS radical cation decolorization assay. Free Radic Biol Med. 1999;26(9–10):1231–7.
29. Elisha C, Bhagwat P, Pillai S. In silico and in vitro analysis of dipeptidyl peptidase-IV and angiotensin-converting enzyme inhibitory peptides derived from milk lactoferrin. Int Dairy J. 2025;160:106092. https://doi.org/10.1016/j.idairyj.2024.106092.
30. Farag YM, Horro C, Vaudel M, Barsnes H. PeptideShaker online: a user-friendly web-based framework for the identification of mass spectrometry-based proteomics data. J Proteome Res. 2021;20(12):5419–23.
31. Liu C, Guo Z, Yang Y, Hu B, Zhu L, Li M, Gu Z, Xin Y, Sun H, Guan Y, Zhang L. Identification of dipeptidyl peptidase-IV inhibitory peptides from yak bone collagen by in silico and in vitro analysis. Eur Food Res Technol. 2022;248(12):3059–69. https://doi.org/10.1007/s00217-022-04111-x.
32. Olsen TH, Yesiltas B, Marin FI, Pertseva M, García-Moreno PJ, Gregersen S, Overgaard MT, Jacobsen C, Lund O, Hansen EB. AnOxPePred: using deep learning for the prediction of antioxidative properties of peptides. Sci Rep. 2020;10(1):21471.
33. Kumar R, Chaudhary K, Singh Chauhan J, Nagpal G, Kumar R, Sharma M, Raghava GP. An in silico platform for predicting, screening and designing of antihypertensive peptides. Sci Rep. 2015;5(1):1–10.
34. Charoenkwan P, Nantasenamat C, Hasan MM, Moni MA, Lio P, Manavalan B, Shoombuatong W. StackDPPIV: A novel computational approach for accurate prediction of dipeptidyl peptidase IV (DPP-IV) inhibitory peptides. Methods. 2022;204:189–98. https://doi.org/10.1016/j.ymeth.2021.12.001.
35. Lear S, Cobb SL. Pep-Calc. com: a set of web utilities for the calculation of peptide and peptoid properties and automatic mass spectral peak assignment. J Comput Aided Mol Des. 2016;30:271–7. https://doi.org/10.1007/s10822-016-9902-7.
36. Iram D, Sansi MS, Zanab S, Vij S, Ashutosh, Meena S. In silico identification of antidiabetic and hypotensive potential bioactive peptides from the sheep milk proteins—a molecular docking study. J Food Biochem. 2022;46(11):e14137. https://doi.org/10.1111/jfbc.14137.
37. Gu Y, Li X, Qi X, Ma Y, Chan ECY. In silico identification of novel ACE and DPP-IV inhibitory peptides derived from buffalo milk proteins and evaluation of their inhibitory mechanisms. Amino Acids. 2023;55(2):161–71.
38. Ampitiya AGDM, Gonapinuwala ST, Fernando CAN, de Croos MDST. Extraction and characterisation of type I collagen from the skin offcuts generated at the commercial fish processing centres. J Food Sci Technol. 2023;60(2):484–93. https://doi.org/10.1007/s13197-022-05630-x.
39. Zhang N, Guo S, Zheng Y, Li W. Isolation and characterisation of acid soluble collagens and pepsin soluble collagens from Eel (Anguilla japonica Temminck et Schlegel) skin and bone. Foods. 2025;14(3):502. . https://www.mdpi.com/2304-8158/14/3/502
40. Iswariya S, Velswamy P, Uma TS. Isolation and characterization of biocompatible collagen from the skin of Puffer Fish (Lagocephalus inermis). J Polym Environ. 2018;26(5):2086–95. . https://doi.org/10.1007/s10924-017-1107-1

41. Song H, Yin B, Jiang B, Mi L, Cui C, Su W, Bai N. Characterization and biological performance of anglerfish collagen and bovine collagen. Appl Biochem Biotechnol. 2025;197(11):7431–49. . https://doi.org/10.1007/s12010-025-05407-w
42. Zhang X, Wang J, Zhang Q, Fan Y, Zhang H, Ahmad K, Hou H. Distribution, typical structure and self-assembly properties of collagen from fish skin and bone. Molecules. 2023;28(18):6529. . https://www.mdpi.com/1420-3049/28/18/6529
43. Sousa RO, Alves AL, Carvalho DN, Martins E, Oliveira C, Silva TH, Reis RL. Acid and enzymatic extraction of collagen from Atlantic cod (Gadus Morhua) swim bladders envisaging health-related applications. J Biomater Sci Polym Ed. 2020;31(1):20–37.
44. Ishak NH, Shaik MI, Yellapu NK, Howell NK, Sarbon NM. Purification, characterization and molecular docking study of angiotensin-I converting enzyme (ACE) inhibitory peptide from shortfin scad (Decapterus macrosoma) protein hydrolysate. J Food Sci Technol. 2021;58(12):4567–77. https://doi.org/10.1007/s13197-020-04944-y.
45. Thuanthong M, De Gobba C, Sirinupong N, Youravong W, Otte J. Purification and characterization of angiotensin-converting enzyme-inhibitory peptides from Nile tilapia (Oreochromis niloticus) skin gelatine produced by an enzymatic membrane reactor. J Funct Foods. 2017;36:243–54. https://doi.org/10.1016/j.jff.2017.07.011.
46. Guo L, Harnedy PA, Zhang L, Li B, Zhang Z, Hou H, Zhao X, FitzGerald RJ. In vitro assessment of the multifunctional bioactive potential of Alaska pollock skin collagen following simulated gastrointestinal digestion. J Sci Food Agric. 2015;95(7):1514–20. https://doi.org/10.1002/jsfa.6854.
47. Luo J, Yao X, Soladoye OP, Zhang Y, Fu Y. Phosphorylation modification of collagen peptides from fish bone enhances their calcium-chelating and antioxidant activity. LWT. 2022;155:112978. https://doi.org/10.1016/j.lwt.2021.112978.
48. Ahn C-B, Kim J-G, Je J-Y. Purification and antioxidant properties of octapeptide from salmon byproduct protein hydrolysate by gastrointestinal digestion. Food Chem. 2014;147:78–83. https://doi.org/10.1016/j.foodchem.2013.09.136.
49. Weng W, Tang L, Wang B, Chen J, Su W, Osako K, Tanaka M. Antioxidant properties of fractions isolated from blue shark (Prionace glauca) skin gelatin hydrolysates. J Funct Foods. 2014;11:342–51. https://doi.org/10.1016/j.jff.2014.10.021.
50. Nurdiani R, Vasiljevic T, Yeager T, Singh TK, Donkor ON. Bioactive peptides with radical scavenging and cancer cell cytotoxic activities derived from Flathead (Platycephalus fuscus) by-products. Eur Food Res Technol. 2017;243(4):627–37. https://doi.org/10.1007/s00217-016-2776-z.
51. Hajfathalian M, Ghelichi S, García-Moreno PJ, Moltke Sørensen A-D, Jacobsen C. Peptides: production, bioactivity, functionality, and applications. Crit Rev Food Sci Nutr. 2018;58(18):3097–129.
52. Xie Z, Wang X, Yu S, He M, Yu S, Xiao H, Song Y. Antioxidant and functional properties of cowhide collagen peptides. J Food Sci. 2021;86(5):1802–18. https://doi.org/10.1111/1750-3841.15666.
53. Bordbar S, Ebrahimpour A, Zarei M, Abdul Hamid A, Saari N. Alcalase-generated proteolysates of stone fish (Actinopyga lecanora) flesh as a new source of antioxidant peptides. Int J Food Prop. 2018;21(1):1541–59.
54. Najafian L, Babji AS. Fractionation and identification of novel antioxidant peptides from fermented fish (pekasam). J Food Meas Charact. 2018;12(3):2174–83. https://doi.org/10.1007/s11694-018-9833-1.
55. Rajapakse N, Mendis E, Jung W-K, Je J-Y, Kim S-K. Purification of a radical scavenging peptide from fermented mussel sauce and its antioxidant properties. Food Res Int. 2005;38(2):175–82. https://doi.org/10.1016/j.foodres.2004.10.002.
56. Wardani DW, Ningrum A, Manikharda, Vanidia N, Munawaroh HSH, Susanto E, Show P-L. In silico and in vitro assessment of yellowfin tuna skin (Thunnus albacares) hydrolysate antioxidation effect. Food Hydrocoll Health. 2023;3:100126. https://doi.org/10.1016/j.fhfh.2023.100126.
57. Auwal SM, Zainal Abidin N, Zarei M, Tan CP, Saari N. Identification, structure-activity relationship and in silico molecular docking analyses of five novel angiotensin I-converting enzyme (ACE)-inhibitory peptides from stone fish (Actinopyga lecanora) hydrolysates. PLoS ONE. 2019;14(5):e0197644. https://doi.org/10.1371/journal.pone.0197644.
58. Munawaroh HSH, Gumilar GG, Berliana JD, Aisyah S, Nuraini VA, Ningrum A, Susanto E, Martha L, Kurniawan I, Hidayati NA, Koyande AK, Show P-L. In silico proteolysis and molecular interaction of tilapia (Oreochromis niloticus) skin collagen-derived peptides for environmental remediation. Environ Res. 2022;212:113002. https://doi.org/10.1016/j.envres.2022.113002.
59. Ye M, Zhang C, Zhu L, Jia W, Shen Q. Yak (Bos grunniens) bones collagen-derived peptides stimulate osteoblastic proliferation and differentiation via the activation of Wnt/β-catenin signaling pathway. J Sci Food Agric. 2020;100(6):2600–9. https://doi.org/10.1002/jsfa.10286.
60. Yamakura F, Ikeda K. Modification of tryptophan and tryptophan residues in proteins by reactive nitrogen species. Nitric Oxide. 2006;14(2):152–61. https://doi.org/10.1016/j.niox.2005.07.009.
61. Ashok N, Aparna H. Empirical and bioinformatic characterization of buffalo (Bubalus bubalis) colostrum whey peptides & their angiotensin I-converting enzyme inhibition. Food Chem. 2017;228:582–94. https://doi.org/10.1016/j.foodchem.2017.02.032.
62. Nongonierma AB, FitzGerald RJ. Dipeptidyl peptidase IV inhibitory and antioxidative properties of milk protein-derived dipeptides and hydrolysates. Peptides. 2013;39:157–63. https://doi.org/10.1016/j.peptides.2012.11.016.
63. Li Y, Zhang F, Gong J, Peng C. Two novel dipeptidyl peptidase-IV (DPP-IV) inhibitory peptides identified from truffle (Tuber sinense) by peptidomics, in silico, and molecular docking analysis. J Food Compos Anal. 2023;121:105384. https://doi.org/10.1016/j.jfca.2023.105384.
64. Renjuan L, Xiuli Z, Liping S, Yongliang Z. Identification, in silico screening, and molecular docking of novel ACE inhibitory peptides isolated from the edible symbiot Boletus griseus-Hypomyces chrysospermus. LWT. 2022;169:114008.
65. Li Y, Li J, Cheng C, Zheng Y, Li H, Zhu Z, Yan Y, Hao W, Qin N. Study on the in silico screening and characterization, inhibition mechanisms, Zinc-chelate activity, and stability of ACE-inhibitory peptides identified in naked oat bran albumin hydrolysates. Foods. 2023;12(11):2268. . https://www.mdpi.com/2304-8158/12/11/2268
66. Xu Q, Zheng L, Huang M, Zhao M. Collagen derived Gly-Pro-type DPP-IV inhibitory peptides: structure-activity relationship, inhibition kinetics and inhibition mechanism. Food Chem. 2024;441:138370. . https://doi.org/10.1016/j.foodchem.2024.138370

Publisher's Note